

Chemical Vapour Deposition of Pyrolytic Carbon from Impinging Jets

S. Eroglu^{a*} & B. M. Gallois^b

^aTUBITAK-Marmara Research Center, Materials Research Dept., P.K. 21, 41470 Gebze-Kocaeli, Turkey

^bStevens Institute of Technology, Dept. Materials Science and Engineering, Hoboken, NJ 07030, USA

(Received 24 May 1995; accepted 28 June 1995)

Abstract: Pyrolytic carbon coatings were deposited on a graphite substrate by chemical vapour deposition technique from impinging jets of ethylene gas. The growth and structure of the coatings were investigated as a function of gas flow velocity. The deposition rate of the coatings increased linearly with the square root of gas velocity or flow rate of ethylene. This behaviour was explained by a mass-transport theory. The coatings exhibited cone-like morphology at low gas velocities and cauliflower-like morphology at high gas velocities. Textural analyses revealed that all the coatings were preferentially oriented in the $\langle 001 \rangle$ direction perpendicular to the substrate. © 1996 Elsevier Science Limited and Techna S.r.l.

1 INTRODUCTION

Most chemical vapour deposition reactors (CVD) operate at low Reynolds numbers ($Re = Ud/\nu$, where U is the gas flow velocity, d is the diameter of the reactor and ν is the kinematic viscosity) or low gas flow velocities. Typical Reynolds numbers are of the order of 10. One of the disadvantages of operating at low gas flow velocities is that flow, especially in cold-wall reactors where there is a steep temperature gradient between the reactor wall and the substrate, is dominated by natural convections leading to flow instabilities which produce non-uniform coatings. In addition, deposition rate increases, especially in mass-transport limited regime, because boundary layer through which gas phase species must diffuse from the gas phase to growth surface decreases with increasing flow velocities. Deposition at high flow velocities may produce coatings with better properties. Deposition time can be reduced, thus reducing surface imperfections and preventing interfacial reactions leading to the formation of brittle products between coating and substrate.

Impinging reactive jets have been used for the chemical vapour deposition of SiC whiskers,¹ boron² and SnO₂³ coatings. It has been shown that the growth rate of SiC whiskers and boron coatings increased with gas velocity and high quality SnO₂ films without any gas-borne particulates were prepared from high-velocity gas stream. In the present study, chemical vapour deposition of pyrolytic carbon coatings from impinging jets was investigated as a function of flow velocity of the reactive gas.

Pyrolytic carbon coatings synthesized by chemical vapour deposition (CVD) technique have been used in many areas ranging from nuclear industry⁴ to bioengineering.⁵ There have been extensive studies⁶ on the relationship between structure of pyrolytic carbon and CVD deposition conditions. No studies have been reported on the chemical vapour deposition of pyrolytic carbon coatings from impinging gas jets.

2 EXPERIMENTAL

The deposition cell is represented schematically in Fig. 1. The stream of ethylene gas was introduced

*To whom correspondence should be addressed.

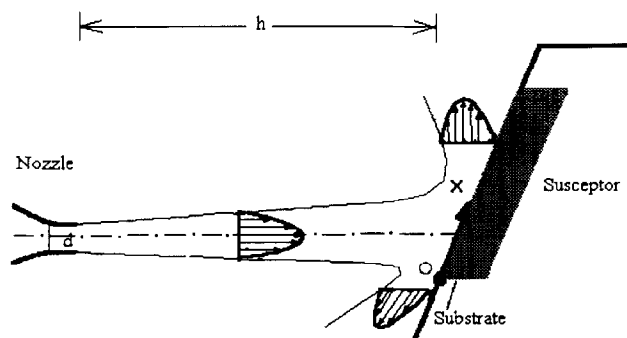


Fig. 1. A schematic diagram of the deposition cell.

in a stainless steel conical nozzle with an exit diameter (d) of 0.13 cm. The jet stream impinged on a graphite substrate of 1.8 cm diameter. The nozzle was aimed at the leading edge of the substrate which was inclined 45° to the nozzle axis, as seen in Fig. 1. The distance (h) between the nozzle and substrate was fixed at 5 cm.

Prior to deposition, the polycrystalline graphite substrate was polished, cleaned in alcohol in an ultrasonic device and dried. The substrate placed on graphite susceptor was heated by a high frequency generator. The depositions were carried at a temperature of 1400 K and at a pressure of 1 atm for 10 min. The flow rate of ethylene gas was varied from 100 to 800 standard cubic centimeters per min (sccm), corresponding nozzle exit velocities of 122–976 cm/s. Growth rate ($\text{gr}/\text{cm}^2\text{s}$) was determined from the weight change measurements of the substrate before and after the deposition.

For the microstructural analysis, the coatings were cut perpendicular to the deposition surface, mounted in resin and polished by using standard metallographic techniques. The cross-sections of the coatings were examined by a polarized light microscope. The deposit thickness was measured with the microscope on the polished transverse cross-sections of the substrate as a function of diametral distance (X). For X-ray analysis, the coatings deposited at high flow rates were peeled off the graphite substrate. Preferred orientation and X-ray density of the coatings were measured by a parafocusing X-ray diffractometer equipped with a Cu radiation tube. The crystallite size and microstrains were also deduced from the X-ray diffraction profiles of the (001) reflections using the following equation:⁷

$$\beta \cos \Theta / \lambda = 1/L + 4e \sin \Theta / \lambda \quad (1)$$

where λ is the wavelength of the X-rays, Θ is the Bragg angle, L is the crystallite size, e is the microstrain and β is the breadth of a diffraction peak at half-maximum intensity.

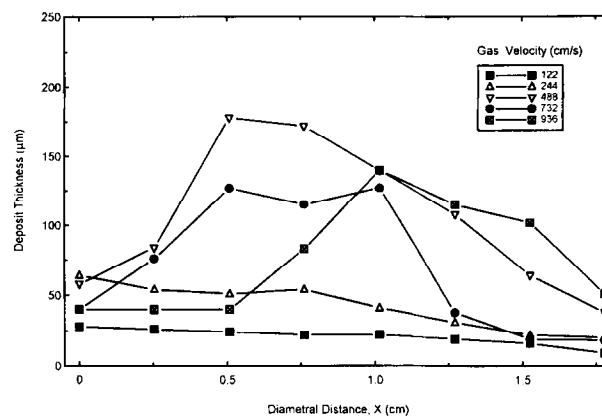


Fig. 2. Effect of gas velocity on deposit thickness along the sample diameter.

3 RESULTS AND DISCUSSION

3.1 Deposit thickness profiles

Figure 2 shows the thickness of pyrolytic carbon deposits as a function of the diametral distance (X) from the leading edge as indicated in Fig. 1 with varying gas velocities. Thickness profiles give information about the characteristics of the jets and the interaction between the jet and the substrate. The coating grown at the lowest gas velocity of 122 cm/s has thickness values about $20 \mu\text{m}$, which slightly decrease with the diametral distance. The thickness profile shifts to higher values when the gas velocity is 244 cm/s, compared to that of the previous coating. The decrease in thickness with the diametral distance is more pronounced. The profiles of the coatings grown at velocities higher than 244 cm/s are different from the others and show a bell-type variation. The thicknesses increase to a maximum value and then decrease as the diametral distance increases. The coating grown at 488 cm/s exhibits the highest maximum thickness, whereas the coatings grown at 732 and 976 cm/s have lower maximum values. It should be noted that the maximum values shift to the higher diametral distances as the gas velocity increases. This behaviour can be attributed to the convective cooling of the lower part of the substrate where the jet first impinges (see Fig. 1), which increases with the gas velocity. The decrease in thickness at upper part of the substrate or higher diametral distances (X) may be the result of the deflection of the jet stream by the substrate and/or because of an increase in the boundary layer through which gaseous species must diffuse to the growth surface.

3.2 Deposition rates

Since the thickness of the coatings is not uniform

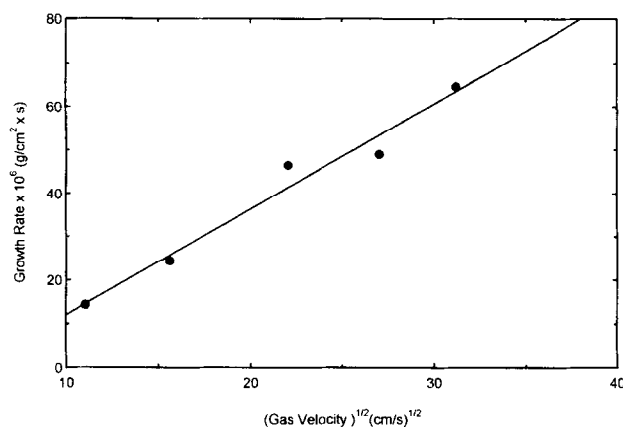


Fig. 3. Growth rate of pyrolytic carbon coatings as a function of square root of gas velocity.

across the substrate, the deposition rates are calculated by dividing weight gain by the substrate surface area and growth time. The results are summarized in Fig. 3 which shows the deposition rate of pyrolytic carbon as a function of gas velocity. It can be seen that growth rate increases with increasing flow velocity. This behaviour can be explained by a mass-transport theory. Since the deposition profiles are greatly affected by the gas flow velocity, it is assumed that the process is mass-transport controlled. In the surface-reaction controlled regime, the dependence of thickness profiles or growth rates on the gas velocity is expected to be weak. At mass-transport limited regime, the deposition rate is proportional to the gas-phase mass transfer coefficient, which is given by⁸

$$h_g = D_g / \delta \quad (2)$$

where D_g is the diffusion coefficient of the reactive gas and δ is the average boundary layer thickness. The diffusion coefficient is given by⁹

$$D_g = D_s (T/288.2)^{1.75} 760/P \quad (3)$$

where D_s is the diffusion coefficient at 288.2 K and 760 torr, P is pressure, and T is temperature (K). D_g was calculated to be $1.9 \text{ cm}^2/\text{s}$ for $P=1 \text{ atm}$, $T=1400 \text{ K}$ and $D_s=0.113 \text{ cm}^2/\text{s}$. The average boundary layer (δ) is given by¹⁰

$$\delta = 3.09(vL/U)^{1/2} \quad (4)$$

where v is the kinematic viscosity ($1.41 \text{ cm}^2/\text{s}$ for ethylene at 1400 K), L is the diameter of the substrate (1.8 cm) and U is the main stream flow velocity over the substrate. It is assumed that U is proportional to the nozzle exit velocity. Since v and L are constant, δ is inversely proportional to

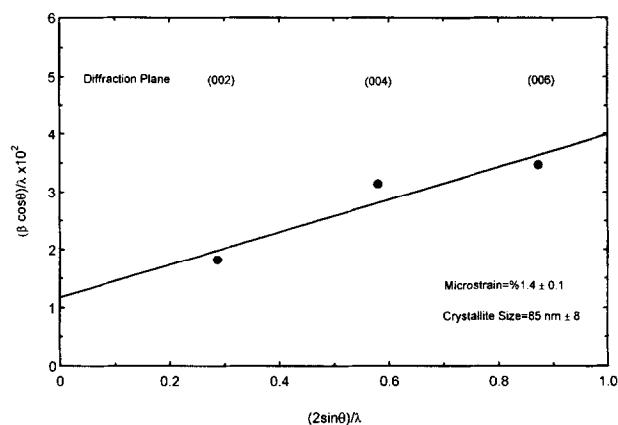


Fig. 4. Variation of $\beta \cos \Theta / \lambda$ with $2 \sin \Theta / \lambda$.

the square root of the gas velocity. (For velocities of 122 and 976 cm/s, the average boundary layer thicknesses are calculated to be 0.45 and 0.17 cm, respectively.) Hence, the combination of eqns (4) and (2) gives

$$\text{Growth rate} \propto U^{1/2} \quad (5)$$

Equation (5) indicates that the growth rate of the pyrocarbon coatings should increase linearly with the square root of gas flow velocity. The experimental results seen in Fig. 3 are found to be in good agreement with the prediction of the mass-transport theory. The increase in growth rate is attributed to the reduction in boundary layer thickness by increasing jet velocity.

3.3 X-ray diffraction analysis

X-ray diffraction studies revealed that the coatings exhibit reflections from (001) crystal planes. This observation indicates that the deposits have a high degree of preferred orientation such that the basal planes of crystallites are aligned parallel to the deposition plane.

Microstrains and crystallite size of the coatings were also determined using eqn (1). For this analysis, only reflections from the (002), (004) and (006) crystal planes were used. Figure 4 shows the variation of $\beta \cos \Theta / \lambda$ with $2 \sin \Theta / \lambda$. The solid line represents the least-square fit to the data. From the slope of the line, the microstrain was calculated to be $1.4\% \pm 0.1$. The crystallite size was also deduced by extrapolating the line to $2 \sin \Theta / \lambda = 0$, where $\beta \cos \Theta / \lambda$ is equal to $1/L$. The crystallite size (L_c) in the direction of c -axis was calculated to be $85 \pm 8 \text{ nm}$.

The $d_{(002)}$ spacing was measured to be 0.342 nm which is much larger than that of highly crystalline pyrolytic graphite (0.336 nm). This suggests that the hexagonal network of atoms of the basal layer

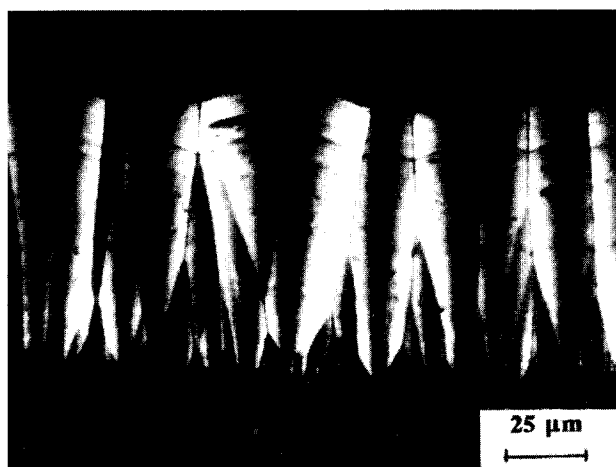


Fig. 5. Cross-sectional view of the pyrocarbon coating grown at a gas velocity of 244 cm/s (polarized light).

was bent or certain atoms of the network were displaced along the *c*-direction. Such distortions contribute heavily to microstrains.

3.4 Morphology

The cross-sectional view of the coating grown at a flow rate of 200 sccm or at a gas velocity of 244 cm/s is shown in Fig. 5. As can be seen from the figure, the microstructure consists of growth cones or columnar grains whose axis is arranged more or less parallel to the growth direction. The cones were observed to be oriented from the substrate. The number of cones decreases as the thickness increases, indicating some cones grow preferentially at the expense of other less favorable cones. The cones with a $\langle 001 \rangle$ preferred orientation survive, whereas the cones of other orientations are gradually buried as the deposition proceeds. This behaviour is commonly observed in

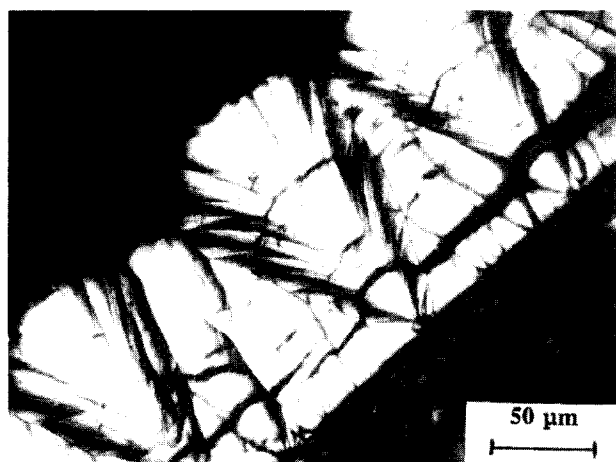


Fig. 6. Cross-sectional view of the pyrocarbon coating grown at a gas velocity of 976 cm/s (polarized light).

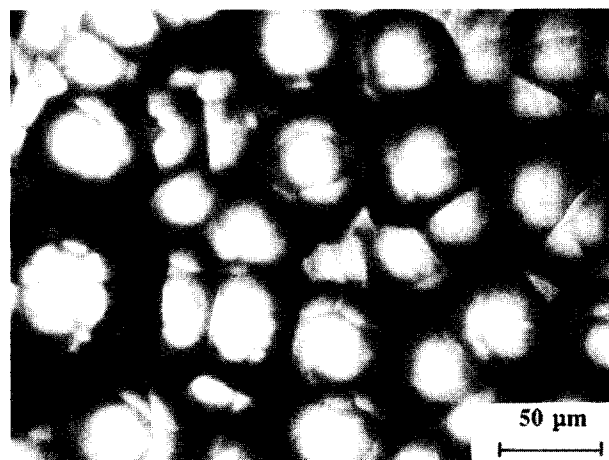


Fig. 7. Surface morphology of the pyrocarbon coating grown at a gas velocity of 976 cm/s (polarized light).

chemically vapour deposited coatings grown at mass-transport limited regime.¹¹ The dark bands in the cones running perpendicular to the substrate are caused by extinction of the polarized light.

Figure 6 shows the cross-sectional view of the coating grown at a flow rate of 800 sccm or a gas velocity of 976 cm/s. This morphology is different from the ones obtained at low jet velocities. It is similar to a cauliflower. The cones are much wider and consist of small branches. The width of crack lines which seem to run parallel to the substrate is larger. Clear breaks of the cones indicate that cracks are formed after the chemical vapour deposition process during cooling stage from the deposition temperature to room temperature. Since the thermal expansion coefficients of pyrolytic carbon in the *c*-direction and *a,b*-directions are different from each other, thermal stresses develop during cooling stage. These stresses cause cracks to form along the direction parallel to the basal planes among which only weak van der Waals bonds exist. No cracks were observed in the direction perpendicular to growth surface. This observation is not surprising because the bond between the C atoms in the basal plane is much stronger.

Surface morphologies of the coatings grown at low gas velocities were observed to be smoother than those grown at high gas velocities. Figure 7 shows the surface morphology of the pyrocarbon coating deposited at a high gas velocity of 976 cm/s. As can be seen, the surface appearance of the coating is rough and exhibits soccer-ball like features.

Although substantial amount of soot formation in the gas phase was observed during the deposition, there were no soot particles incorporated into the deposits as can be seen from the microstructures.

4 CONCLUSIONS

An impinging jet CVD reactor was used to investigate the deposition of pyrolytic carbon as a function of gas flow velocity. Coating uniformity in thickness across the substrate degraded with increasing gas velocity. A mass-transport theory was used to explain the linear increase in growth rate with the square root of the gas velocity. The coatings exhibited growth cones with a $\langle 001 \rangle$ preferred orientation perpendicular to the substrate. The coatings did not contain any soot particles formed in the gas phase.

REFERENCES

1. CHRISTIANSEN, D. E. & VAN ECHOUT, B., Turbulent jets in chemical vapour deposition. *Chemical Engineering Progress*, **84** (1988) 18–22.
2. VANDENBULCKE, L. & VUILLARD, G., Mass transfer, equilibrium and kinetics in the chemical vapour deposition of boron from impinging jets. *J. Electrochem. Soc.*, **124** (1977) 1931–1936.
3. TABATA, O., TANAKA, T., WASEDA, M. & KINUHARA, K., A new CVD method by a reflecting gas stream. In *Proc. 7th Int. Conf. CVD*, ed. T. O. Sedwick & H. Lydtin. Electrochem. Soc. Inc., Princeton, NJ, 1979, pp. 549–562.
4. GUILLERAY, J., LEFEVRE, R. L. R. & PRICE, M. S. T., Pyrocarbon coatings of nuclear fuel particles. In *Chemistry and Physics of Carbon*, Vol. 14, ed. P. L. Walker & P. A. Thrower. Dekker, New York, NY, 1978, pp. 1–108.
5. BOKROS, J. C., LEGRANGE, L. D., SCHOEN, F. L., Control of structure of carbon for use in bioengineering. In *Chemistry and Physics of Carbon*, Vol. 9, ed. P. L. Walker & P. A. Thrower. Dekker, New York, NY, 1972, pp. 103–171.
6. BOKROS, J. C., Deposition, structure and properties of pyrolytic carbon. In *Chemistry and Physics of Carbon*, Vol. 5, ed. P. L. Walker. Dekker, New York, NY, 1969, pp. 1–118.
7. RICKERBY, D. S., BELLAMY, B. A. & JONES, A. M., X-ray diffraction studies of physically vapour deposited coatings. *Surf. Coat. Technol.*, **37** (1989) 111–137.
8. GROVE, A. S., *Physics and Technology of Semiconductor Devices*. John Wiley and Sons, New York, NY, 1967, p. 14.
9. DUSHMAN, S., *Scientific Foundations of Vacuum Technique*. John Wiley and Sons, New York, NY, 1949, pp. 74–77.
10. ECKERT, E. R. G., *Heat and Mass Transfer*. McGraw-Hill Company, New York, NY, 1959, p. 140.
11. EROGLU, S. & GALLOIS, B., Growth and structure of TiC coatings chemically vapour deposited on graphite substrates. *J. Mater. Sci.*, **30** (1995) 1754–1759.